# SUPPORTING INFORMATION

## Using single atoms and/or subnanometric nanoparticles in catalysis or using catalysis for their detection?

### S0. Experimental section

For each Ru/$C_{60}$ ratio studied, the quantities of reactants are detailed hereafter:

D-$Ru_1$-$C_{60}$ 1/1: 30.0 mg (0.10 mmol) of [Ru(COD)(COT)]; 68.5 mg (0.10 mmol) of fullerene $C_{60}$ and 300 mL of $CH_2Cl_2$. Yield: 68.1 mg. Ru: 10.6%

D-Ru-$C_{60}$ 2/1: 80 mg (0.25 mmol) of [Ru(COD)(COT)]; 91.3 mg (0.126 mmol) of fullerene $C_{60}$ and 400 mL of $CH_2Cl_2$. Yield: 100 mg. Ru: 16.7%

D-Ru-$C_{60}$ 5/1: 200 mg (0.63 mmol) of [Ru(COD)(COT)]; 91.3 mg (0.126 mmol) of fullerene $C_{60}$ and 400 mL of $CH_2Cl_2$. Yield:129 mg. Ru: 35.6%

T-$Ru_1$@$C_{60}$ 1/1: 62.5 mg (0.2 mmol) of [Ru(COD)(COT)]; 142.8 mg (0.2 mmol) of fullerene $C_{60}$ and 50 mL of toluene. Yield 116.9 mg. Ru: 9.1 %

T-Ru@$C_{60}$ 5/1: 250 mg (0.8 mmol) of [Ru(COD)(COT)]; 114.2 mg (0.16 mmol) of fullerene $C_{60}$ and 50 mL of toluene. Yield 136.8 mg. Ru: 11.0 %

T-Ru@$C_{60}$ 10/1: 250 mg (0.8 mmol) of [Ru(COD)(COT)]; 57.2 mg (0.08 mmol) of fullerene $C_{60}$ and 50 mL of toluene. Yield 88.9 mg. Ru: 16.6 %

T-Ru@$C_{60}$ 20/1: 250 mg (0.8 mmol) of [Ru(COD)(COT)]; 28.6 mg (0.04 mmol) of fullerene $C_{60}$ and 50 mL of toluene. Yield 58.3 mg. Ru: 20.0 %

T-Ru@$C_{60}$ 40/1: 250 mg (0.8 mmol) of [Ru(COD)(COT)]; 14.3 mg (0.02 mmol) of fullerene $C_{60}$ and 50 mL of toluene. Yield 18.0 mg. Ru: 19.2 %

T-Ru@$C_{60}$ 20/1 50°C: 200 mg (0.64 mmol) of [Ru(COD)(COT)]; 22.9 mg (0.032 mmol) of fullerene $C_{60}$ and 50 mL of toluene. Yield 31.7 mg. Ru: 19.6 %

T-Ru@$C_{60}$ 20/1 100°C: 150 mg (0.47 mmol) of [Ru(COD)(COT)]; 17.1 mg (0.0 mmol) of fullerene $C_{60}$ and 37 mL of toluene. Yield 24.2 mg. Ru: 20.5 %

$T_{95}D_5$-Ru@$C_{60}$ 20/1: 250 mg (0.8 mmol) of [Ru(COD)(COT)]; 28.6 mg (0.04 mmol) of fullerene $C_{60}$, 47.5 mL of toluene and 2.5 mL dichloromethane. Yield 56.7 mg. Ru: 24.4 %

$T_{75}D_{25}$-Ru@$C_{60}$ 20/1: 250 mg (0.8 mmol) of [Ru(COD)(COT)]; 28.6 mg (0.04 mmol) of fullerene $C_{60}$, 37.5 mL of toluene and 12.5 mL dichloromethane. Yield 73.0 mg. Ru: 35.8 %

$T_{50}D_{50}$-Ru@$C_{60}$ 20/1: 250 mg (0.8 mmol) of [Ru(COD)(COT)]; 28.6 mg (0.04 mmol) of fullerene $C_{60}$, 25.0 mL of toluene and 25.0 mL dichloromethane. Yield 80.6 mg. Ru: 36.0 %

$T_{95}M_5$-Ru@$C_{60}$ 20/1: 200 mg (0.64 mmol) of [Ru(COD)(COT)]; 24.1 mg (0.033 mmol) of fullerene $C_{60}$ and 47.5 mL of toluene and 2.5 mL of methanol. Yield 50.0 mg. Ru: 34.7%

$T_{75}M_{25}$-Ru@$C_{60}$ 20/1: 250 mg (0.8 mmol) of [Ru(COD)(COT)]; 28.6 mg (0.04 mmol) of fullerene $C_{60}$, 37.5 mL of toluene and 12.5 mL methanol. Yield 70.0 mg. Ru: 41.6 %

$T_{50}M_{50}$-Ru@$C_{60}$ 20/1: 250 mg (0.8 mmol) of [Ru(COD)(COT)]; 28.6 mg (0.04 mmol) of fullerene $C_{60}$, 25.0 mL of toluene and 25.0 mL methanol. Yield 103.8 mg. Ru: 47.1 %

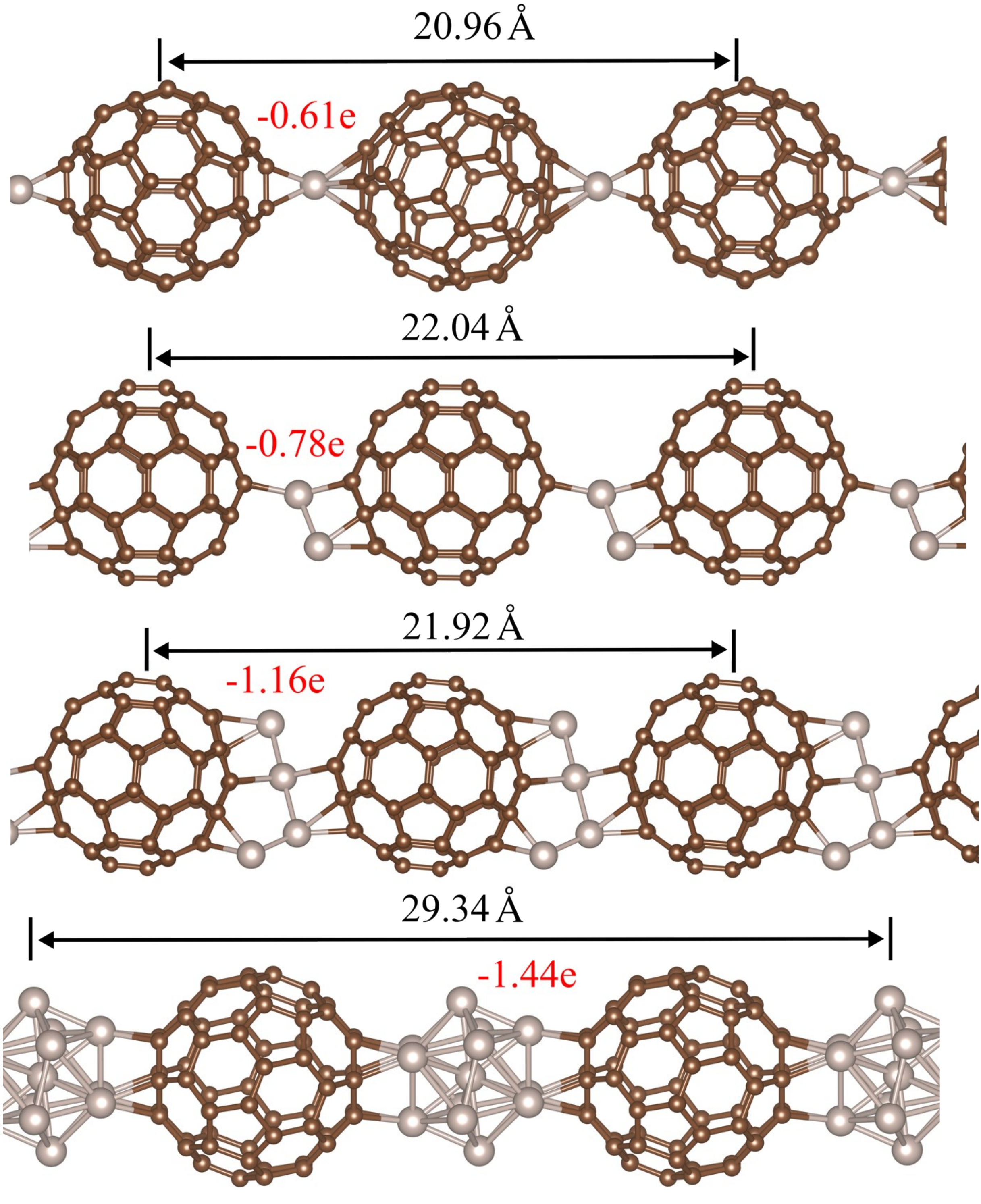


**Figure S1.** Models of polymeric phases for $Ru_1$-$C_{60}$, $Ru_2$-$C_{60}$, $Ru_4$-$C_{60}$, $Ru_{13}$-$C_{60}$ building blocks used for the evaluation of charge transfer and the simulated Pair Distribution Function (PDF), and total charge loss for the corresponding $Ru_n$ cluster.

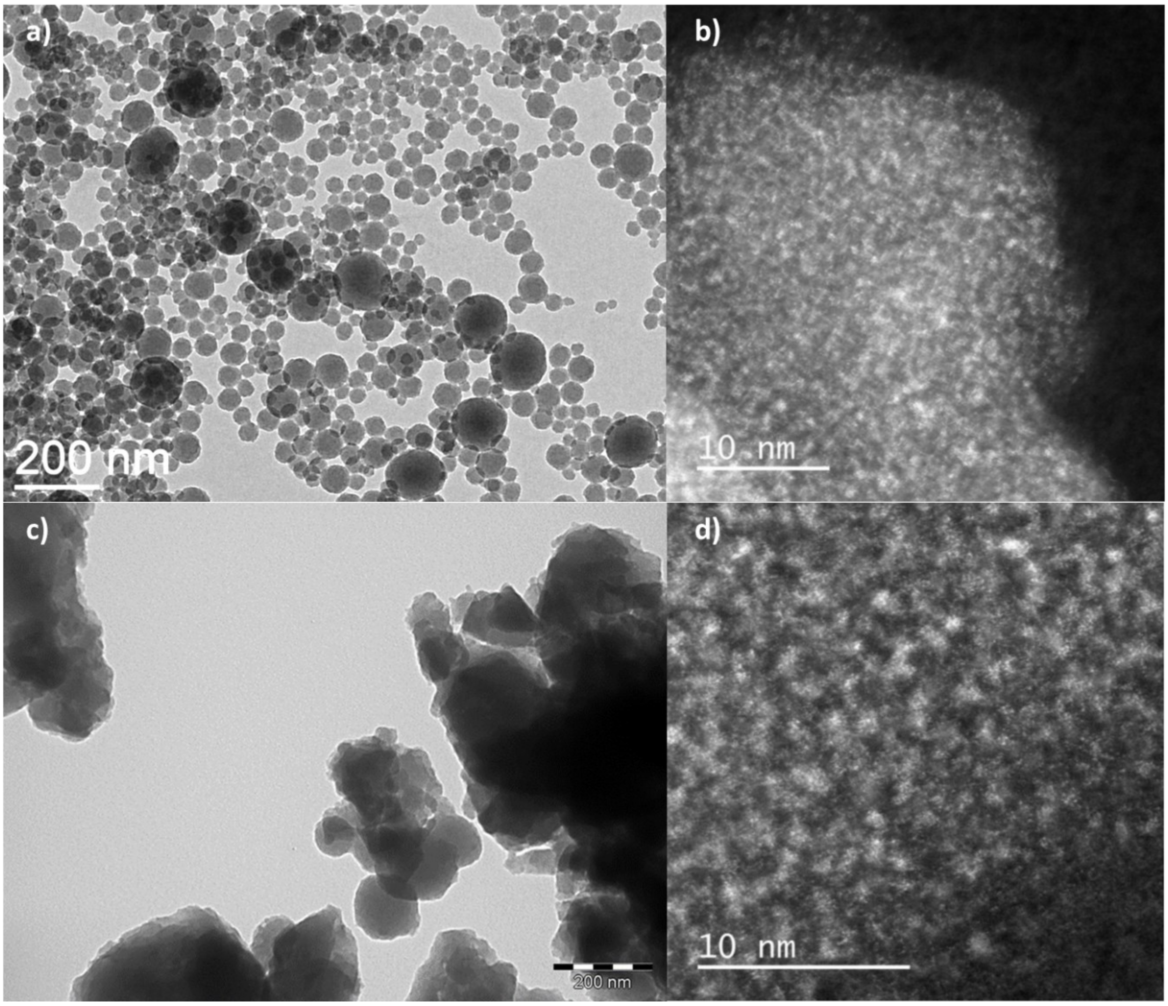


**Figure S2.** a) TEM of D-Ru@$C_{60}$ 1/1; b) STEM-HAADF of D-Ru@$C_{60}$ 1/1; c) TEM of T-Ru@$C_{60}$ 1/1; and d) STEM-HAADF of T-Ru@$C_{60}$ 1/1.

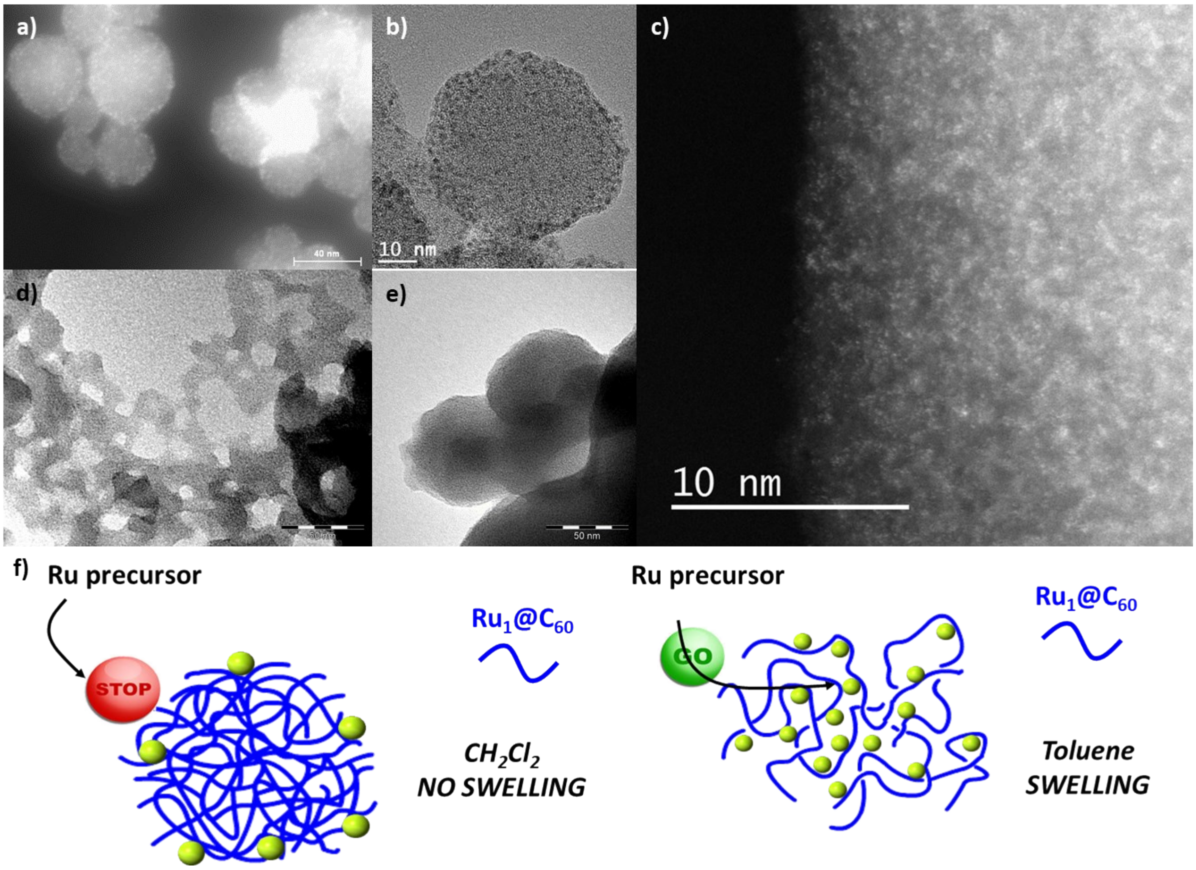


**Figure S3.** a) STEM-HAADF of D-Ru@$C_{60}$ 2/1; b) TEM of D-Ru@$C_{60}$ 2/1; c) STEM-HAADF of T-Ru@$C_{60}$ 1/1; d) and e) TEM of T-Ru@$C_{60}$ 5/1; and f) scheme showing the incorporation of Ru on/in $Ru_1$@$C_{60}$ according to the nature of the solvent.

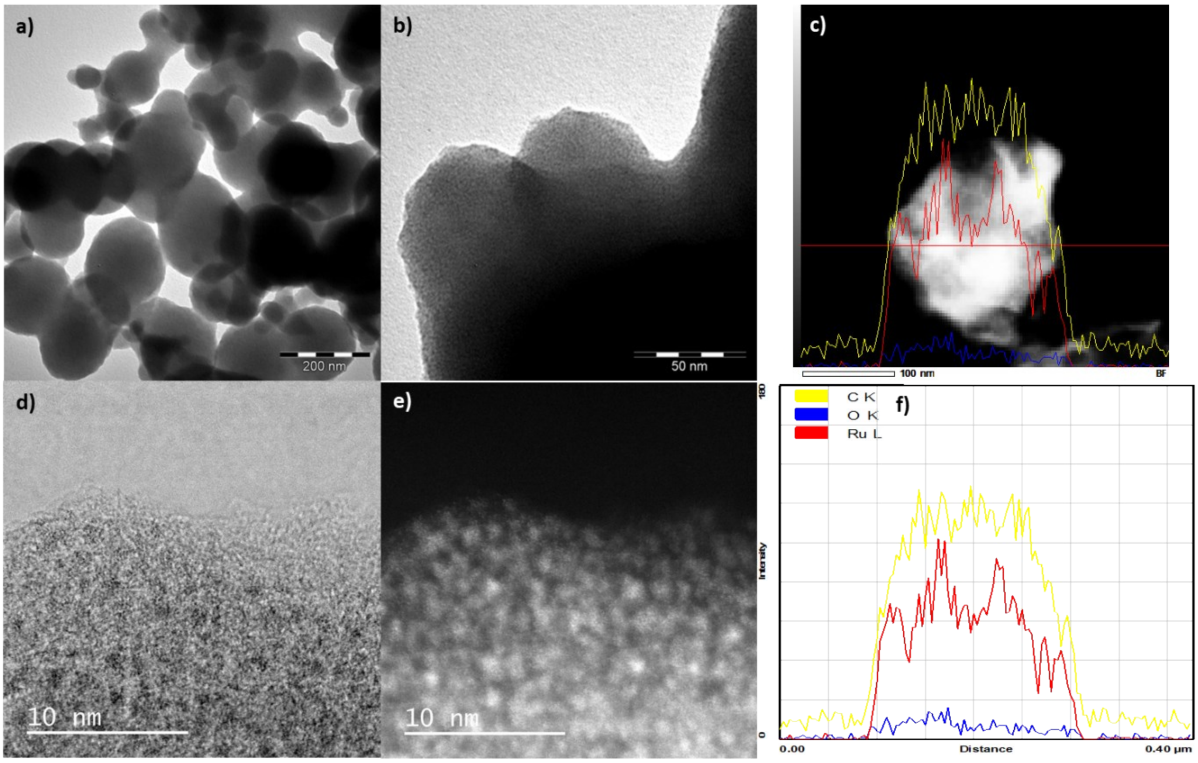


**Figure S4.** TEM, STEM, STEM-HAADF micrographs and EDX mapping of the T-Ru@$C_{60}$ 20/1 sample.

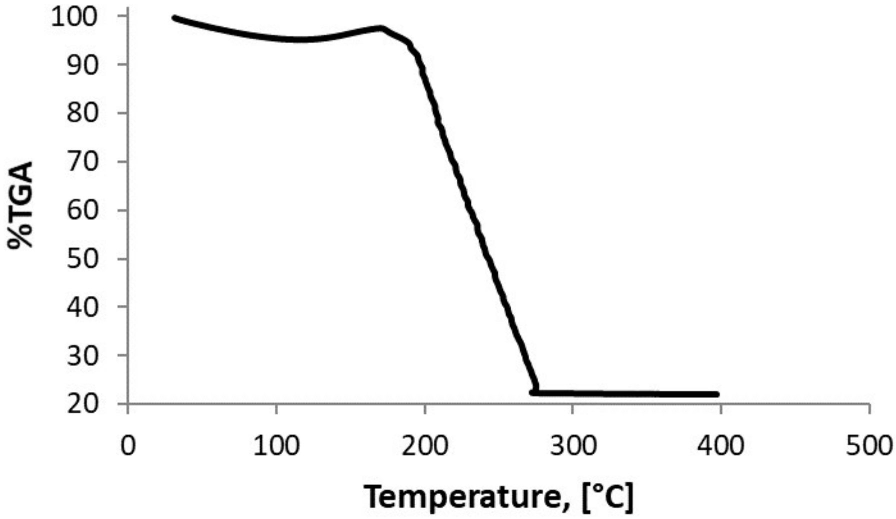


**Figure S5.** Mass loss of T-Ru@$C_{60}$ 10/1 swelled in pure toluene (24 h and then dried at room temperature during 3 days), TG curve measured under nitrogen flow 40 $cm^3$/min.

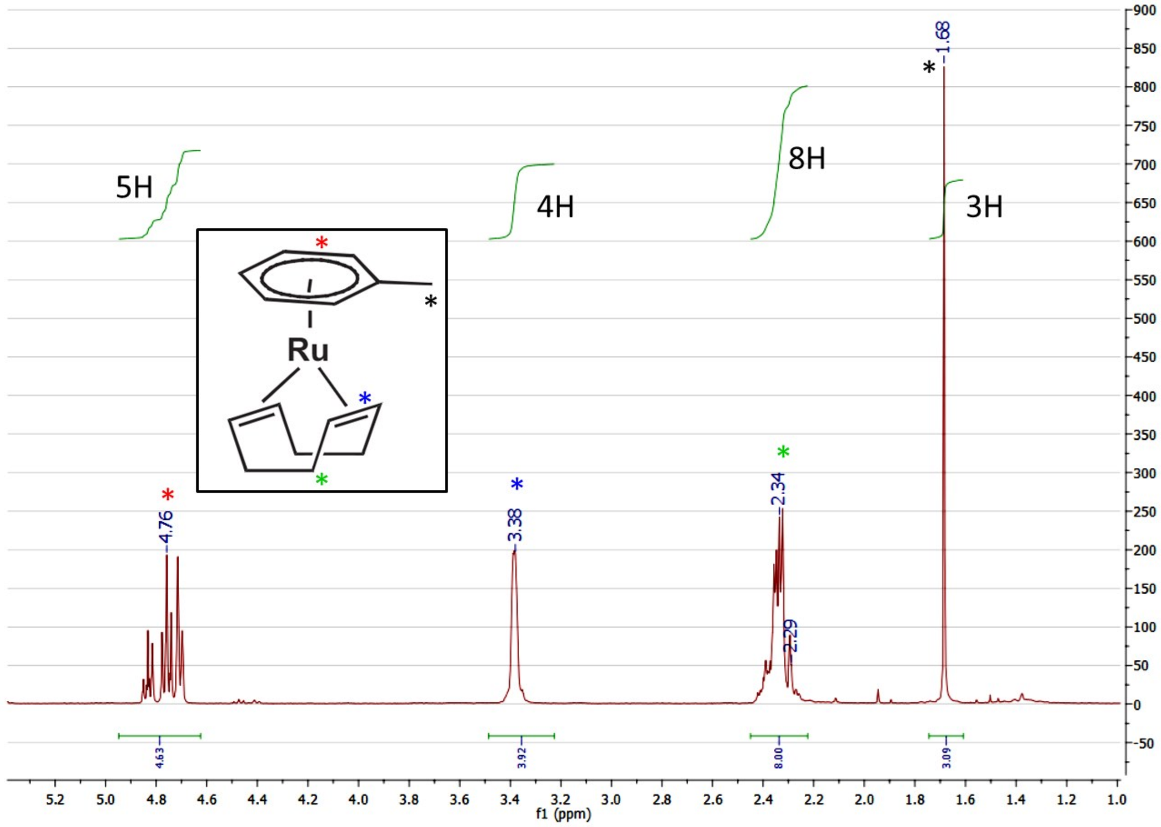


**Figure S6.** [1]H NMR spectrum of (1,5-cyclooctadiene)(toluene)Ru(0) isolated from the yellow filtrates obtained at the end of the reaction of entry 7 of Table 1.

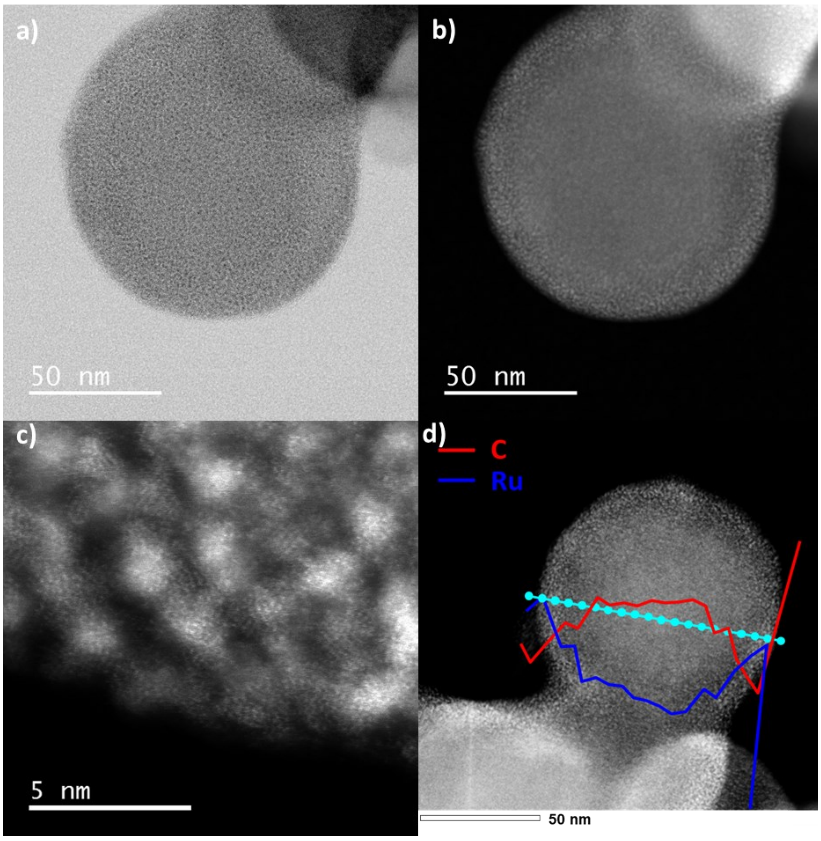


**Figure S7.** a) STEM ; and b-d) STEM-HAADF micrographs of the $T_{95}D_5$-Ru@$C_{60}$ 20/1 sample.

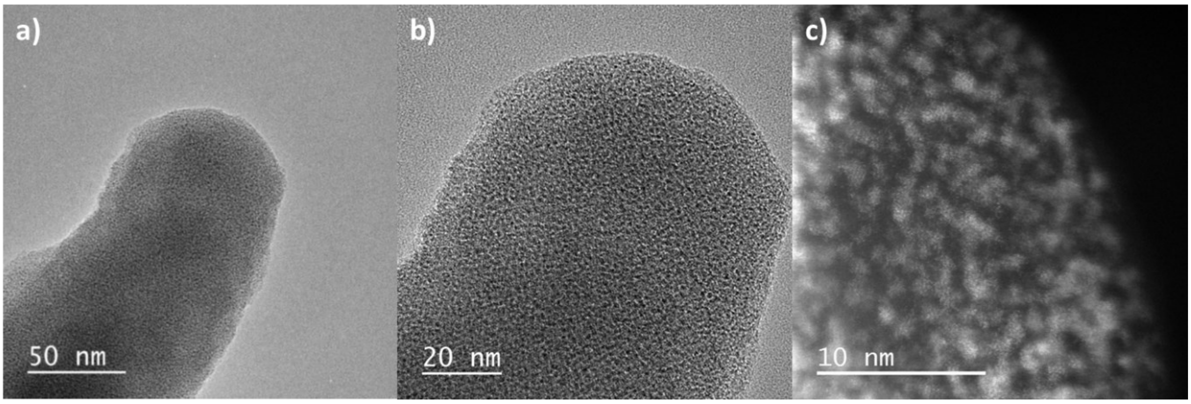


**Figure S8.** a) and b) STEM ; and c) STEM-HAADF micrographs of the $T_{95}M_5$-Ru@$C_{60}$ 20/1 sample.

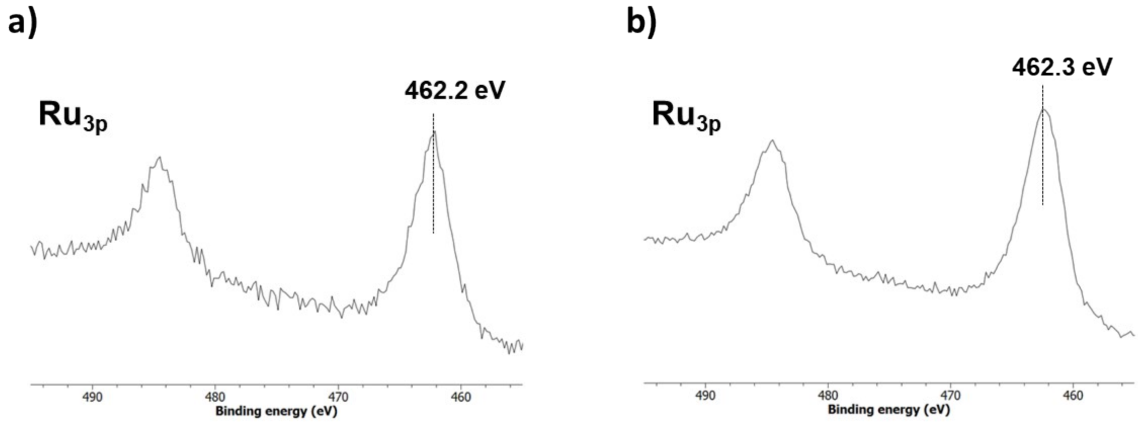


**Figure S9**. $Ru_{3p}$ XPS spectra of a) T-Ru@$C_{60}$ 1/1 ; and b) T-Ru@$C_{60}$ 20/1 samples.

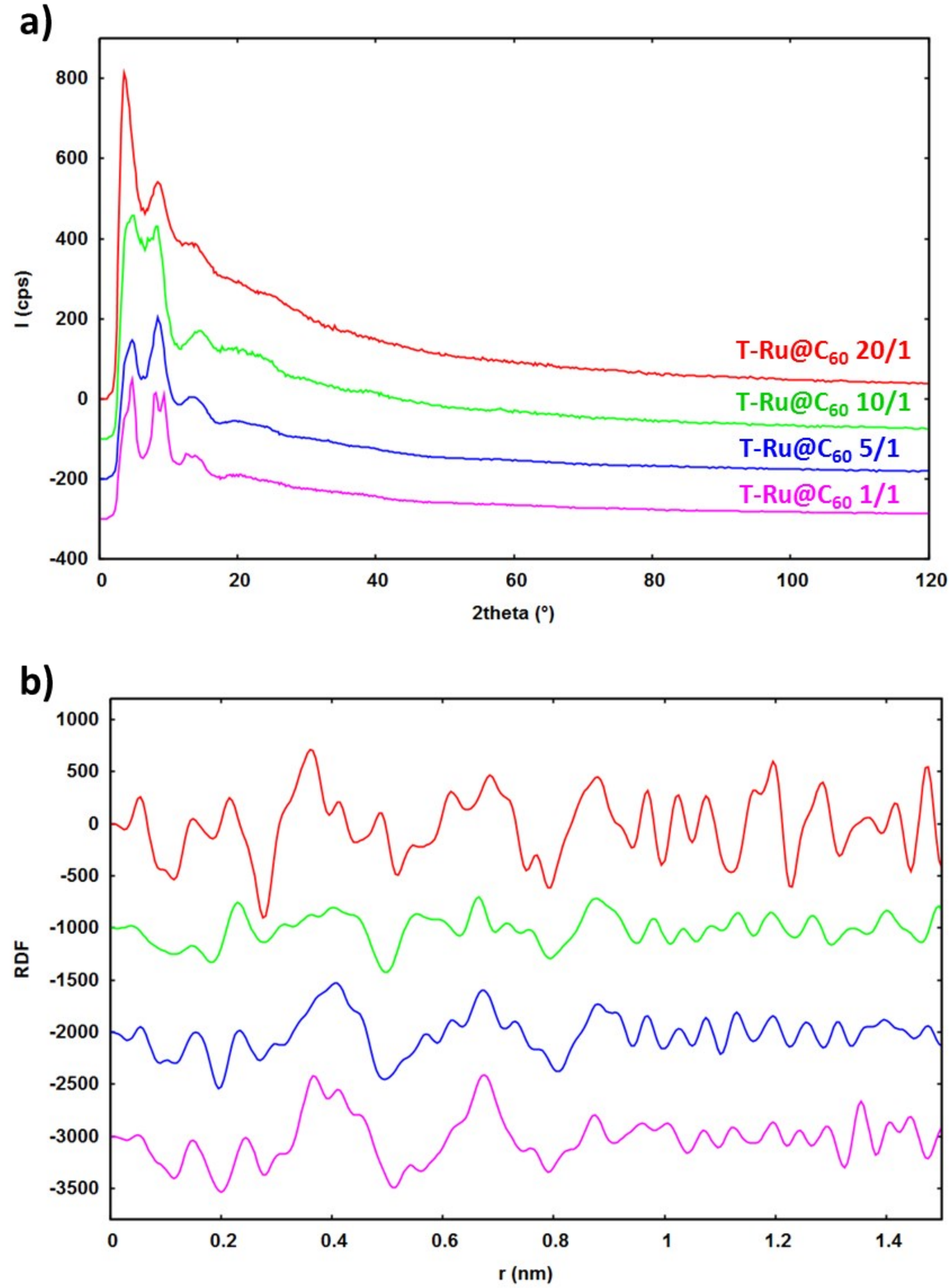


**Figure S10.** a) Diffractograms for T-Ru@$C_{60}$ compounds at different Ru/$C_{60}$ ratio; and b) related PDF.

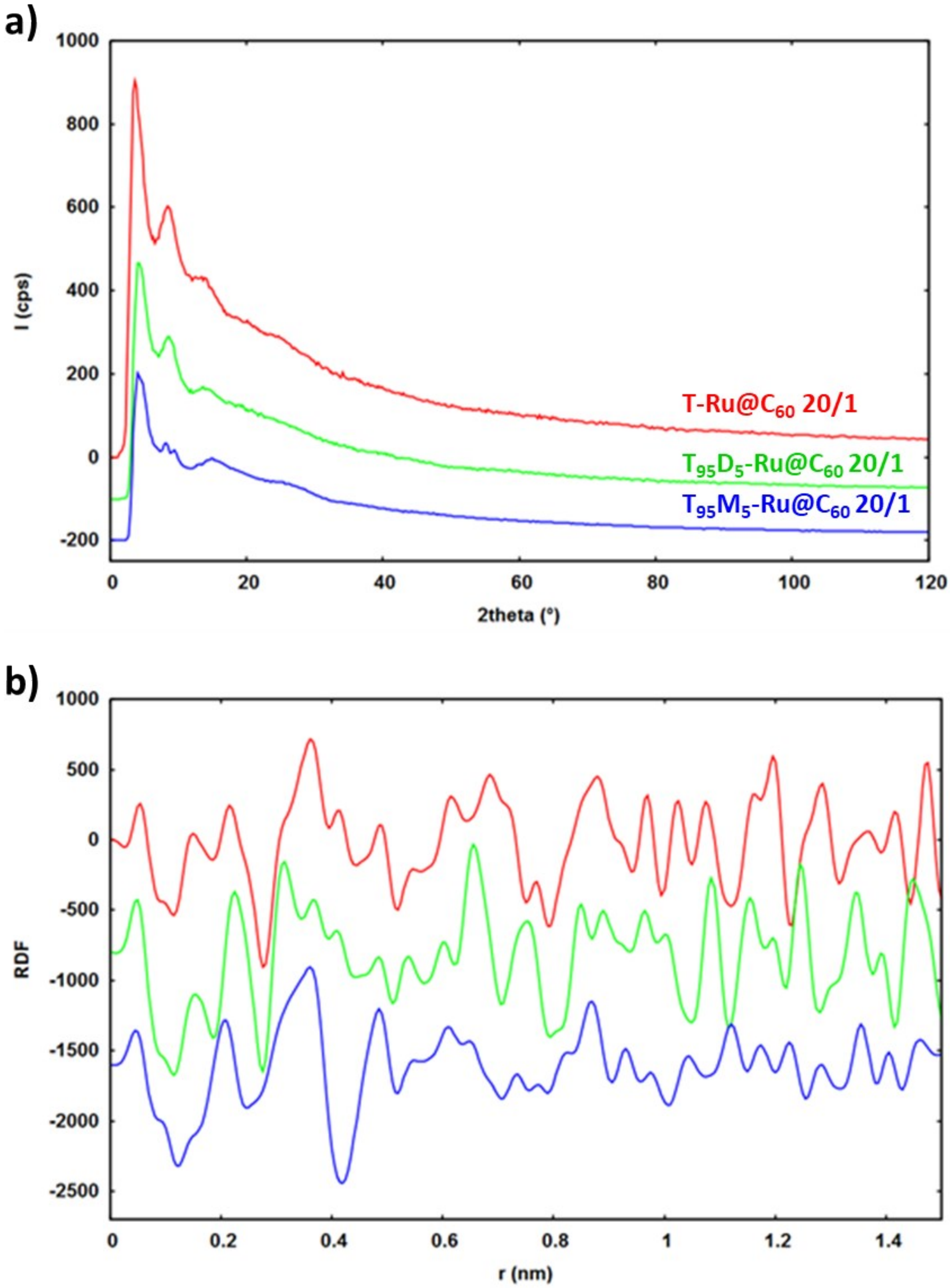


**Figure S11.** a) a) Diffractograms of $T_{95}D_5$-Ru@$C_{60}$, $T_{95}M_5$-Ru@$C_{60}$ and T-Ru@$C_{60}$ samples (Ru/$C_{60}$ = 20/1); and b) related PDF.

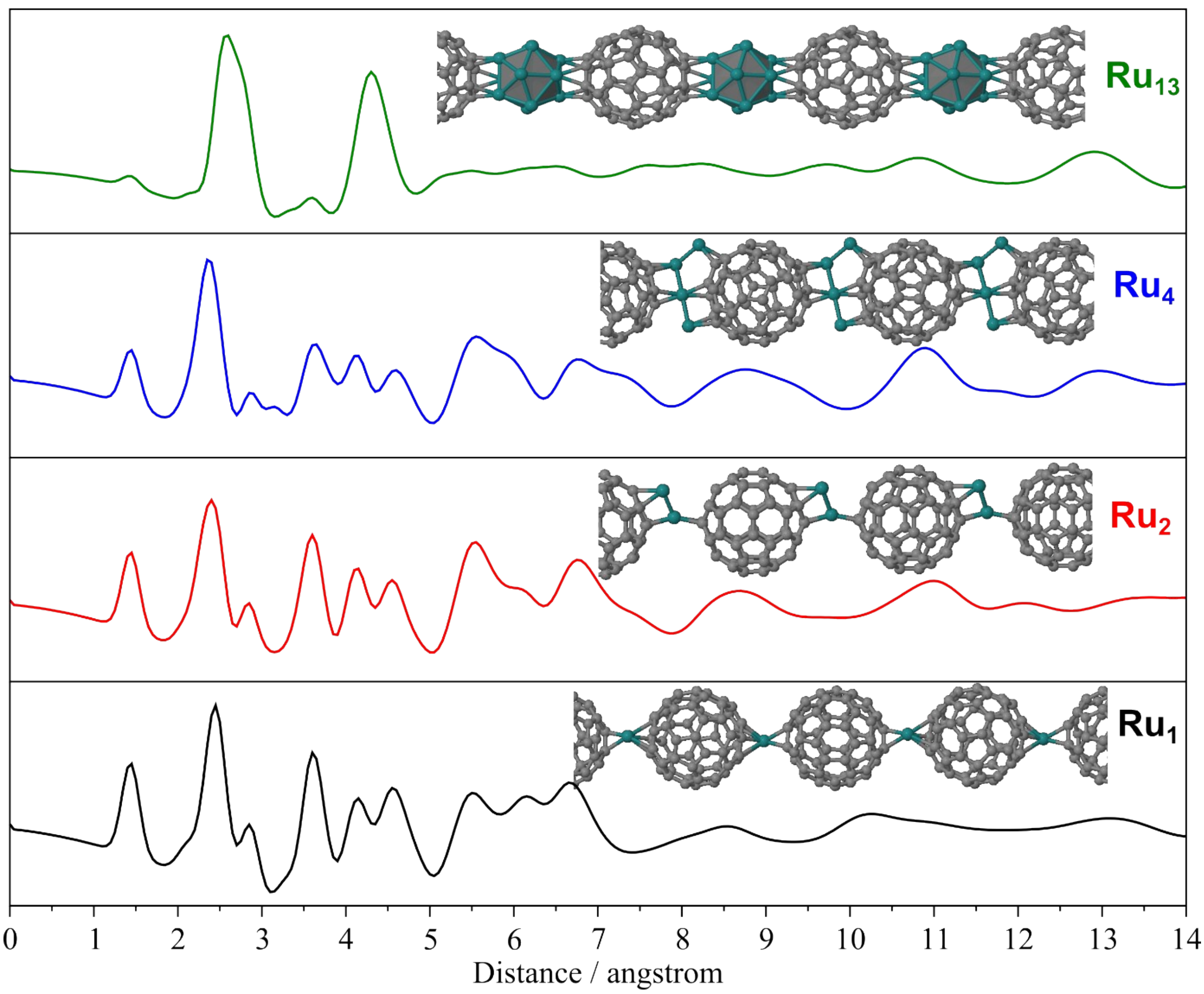


**Figure S12**. Simulated PDF profiles derived from the models optimized at the DFT-PBE level of theory that are shown in Figure S1_DFT. Details regarding such simulations can be found in Refs [1].


[1] a) R. L. McGreevy, L. Pusztai, *Mol. Simul*. **1988**, *1*, 359-367; b) T. Proffen, S. Billinge, *J. Appl. Crystallogr.* **1999**, *32*, 572-575; c) L. Cusinato, I. del Rosal, R. Poteau, *Dalton Trans*. **2017**, *46*, 378-395; d) J. A. Vargas, V. Petkov, E. S. Nouh, R. Ramaamorthy, L.-M. Lacroix, R. Poteau, G. Viau, P. Lecante, R. Arenal, *ACS Nano* **2018**, *12*, 9521-9531